Journal of Water & Health

Journal of Water and Health Vol 21 No 8, 1017 doi: 10.2166/wh.2023.033

Efficient adsorption of tartrazine from an aqueous solution using a low-cost orange peel powder

Amana Tokodne Honorine [a,*], Abia Daouda [a,b], Domga T. [c], Domga Richard [d] and Noumi Guy Bertrand [a]

[a] Department of Chemistry, Faculty of Sciences, University of Ngaoundere, Ngaoundere, Cameroon
[b] Department of Mineral Engineering, School of Chemical Engineering and Mineral Industries, University of Ngaoundere, Ngaoundere, Cameroon
[c] Department of Chemical Engineering, School of Chemical Engineering and Mineral Industries, University of Ngaoundere, Ngaoundere, Cameroon
[d] Department of Applied Chemistry, ENSAI, University of Ngaoundere, Ngaoundere, Cameroon
*Corresponding author. E-mail: honorineamanatokodne@gmail.com

ATH, 0000-0002-6989-6277; DT, 0000-0003-0300-9564; NGB, 0000-0003-2469-6551

ABSTRACT

Orange peel powder was activated using different methods and was used to remove tartrazine (E102) from an aqueous solution. The following three adsorbents were synthethized: orange peel powder activated thermally (POAT), orange peel powder activated with sulfuric acid (POAA), orange peel powder activated with soda (POAS). These adsorbents were then characterized by Fourier Transform Infra-Red Spectrometry (FTIR), Raman spectroscopy, powder X-Ray Diffraction (XRD), and point-of-zero charge. The experimental parameters such as contact time, dose of adsorbent, initial concentration of tartrazine, pH, and temperature were studied. The adsorption capacities of tartrazine for the optimal POAT, POAA, and POAS were found to be 121.74, 122.25, and 116.35 mg/g, respectively. The experimental data were analyzed by Freundlich and Temkin isotherm models, as well as the pseudo-second-order kinetic model.

Key words: adsorbents, adsorption, isotherm, kinetic, tartrazine

HIGHLIGHTS

- Orange peel adsorbents were used for the removal of tartrazine from water.
- The adsorption process followed a pseudo-second-order kinetic model ($R^2 = 0.999$ and 1).
- The adsorption capacity of tartrazine onto the adsorbent depends on the type of activation.
- The adsorption capacity of tartrazine onto the adsorbent depends on parameter studies.
- The effect of many factors on dye adsorption is negligible or little.

GRAPHICAL ABSTRACT

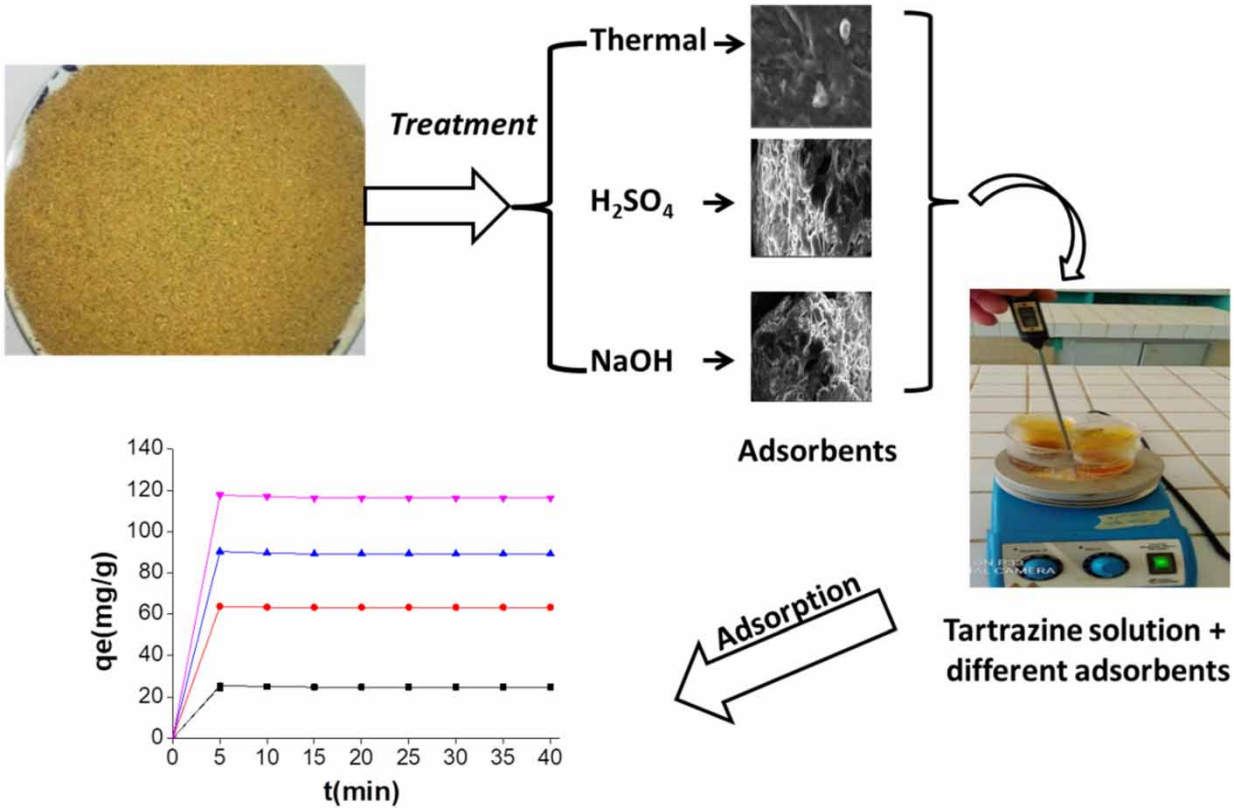

1. INTRODUCTION

Several industrial processes like textiles, rubber, plastics, food products, paper, and leather employ a variety of synthetic product dyes for various applications. These industries produced about 800,000 tons of synthetic dyes annually and 50% of these are azo dyes (Greluk & Hubicki 2011). The azo dyes are molecules with a complex aromatic structure, resistant to temperature, light, and oxidizers (Pearce *et al.* 2003). Tartrazine (E102) is a synthetic azo dye used as a food additive by many industries, especially in the manufacture of food products (juices, ice creams, jams, sauces, yogurt, and cakes), pharmaceuticals (syrup, capsules, and pills), and cosmetics (scent, nail polish, soaps, toothpastes, and shampoos) (Scotter & Castle 2004; Ollemberg 2005; Pereira *et al.* 2006; Kraemer *et al.* 2022). Excessive consumption of this dye beyond 0–7.5 mg/kg which is the acceptable daily dose leads to cancer, asthma, infertility, visual disturbances, and rhinitis in the long term (Panel & Chain 2009). This dye used by the industries is subsequently rejected in the water collection basin (Ramuthai *et al.* 2009). Many works have been achieved in order to remove the color and other pollutants by ozonation, the addition of reducing agents, membrane filtration, ion-exchange, the Fenton method, and adsorption methods. The latter has many advantages like simplicity and efficacy but its utilization is limited due to its expensive cost. For this, many adsorbents have been prepared like activated carbon[13], clay, alumina, silicon oxide, and food residues were used for the removal of color by activating it in three ways for adsorption of E102. Among various adsorbents, one of the most explored studied adsorbents is activated carbon. Many researchers have explored the feasibility of low-cost substitutes such as orange peel, rice husk, and used coffee leaves for the elimination of dyes from aqueous solutions (Arami *et al.* 2006).

The present study addresses the use of orange peel powder as an adsorbent for the elimination of tartrazine, an azo dye from an aqueous solution. The raw material (orange peel) is a solid by-product or waste produced in large quantities in many countries. A thorough literature search revealed that there is presently no research on the use of orange peel powder for the elimination of tartrazine. According to the literature, the chemical modification of raw materials can significantly increase the elimination capacity of dyes in an aqueous solution (Malik *et al.* 2007). Therefore, in this study, the potential of thermally and chemically modified orange peel powder for the elimination of tartrazine in aqueous solutions

is studied. The prepared material was characterized to get information on the morphology and then the effect of operating parameters on the elimination of the azo dyes was studied.

2. MATERIALS AND METHODS

2.1. Preparation of adsorbents

Orange peels were collected from Ngaoundere, Cameroon, washed using distilled water, and then dried at 45 °C (Benaïssa & Elouchdi 2011) in an oven. After drying, peels were crushed and sieved (1 mm), and a part of them is subjected to thermal activation (POAT), chemical activation (sulfuric acid (POAA)), and soda activation (POAS). For thermal activation, these powders were calcined at 500 °C in a muffle oven for 1 h. For acid and soda activation, respectively, the as-prepared orange peel powders were impregnated with a solution of sulfuric acid (H_2SO_4) and soda in an oven at 105 °C and at ambient temperature, respectively, and then washed at neutral pH with distilled water before being dried between 40–50 °C and at 105 °C, at a constant weight.

2.2. Preparation of tartrazine solution

Tartrazine is an anionic dye with a molecular formula $C_{16}H_9N_4Na_3O_9S_2$ (Figure 1). For the study, 1 g of this dye was dissolved in distilled water to prepare the stock solution and then diluted to an appropriate concentration for each test.

2.3. Determination of wavelengths of tartrazine

UV–Visible absorption spectrum of tartrazine (E102), of concentration 60 mg/L, was obtained by spectral scanning, between 400 and 520 nm (Figure 2). The spectrum shows a maximum wavelength of tartrazine at 462 nm.

2.4. Adsorbent characterization

The dry matter provides information on the real mass of material that is brought in contact with the solution, while the water content makes it possible to determine the residual humidity of our material samples. As for the ash tenor, it allows us to know the mineral, inert, and unusable portion of the orange peel.

Iodine Index is a relative indicator of the porosity of adsorbents. It measures the micropores contained and accessible to small molecules; it was identified by the method used by Benamraoui (2014). Specific surface area determines the area available by methylene blue (MB) for the adsorption of a monomolecular layer from the outer and inner surfaces of fine particles of a solid suspended in the aqueous medium.

Fourier Transform Infra-Red (FTIR) was utilized to determine functional groups present in the materials. Using a mixture of potassium bromide and orange peel powders, a ball was made and was scanned in a wave-number scale of 400–4,000 cm^{-1}. Field emission scanning electron microscopy (FE-SEM) characterization was carried out to acquire the structure and morphology of POAT, POAA, and POAS. A Carl Zeiss Supra 55VP microscope equipped with an accelerating voltage of 0.1–30 kV was used for this purpose.

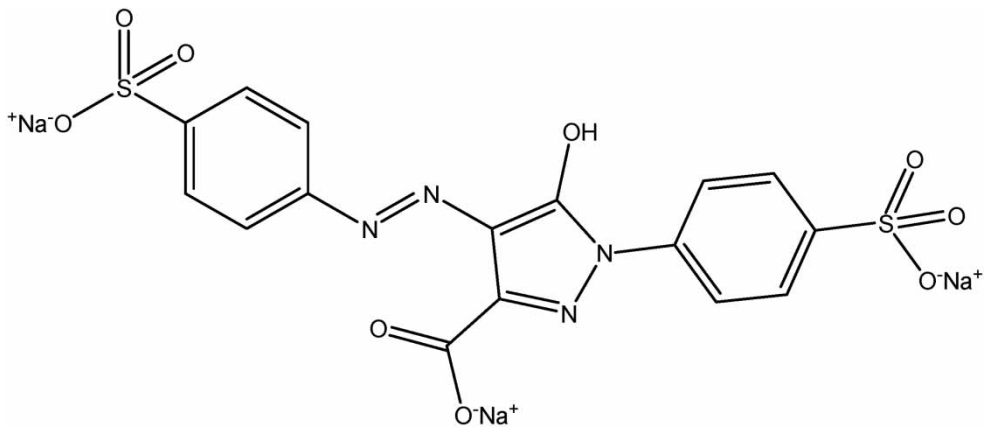

Figure 1 | Chemical structure of tartrazine.

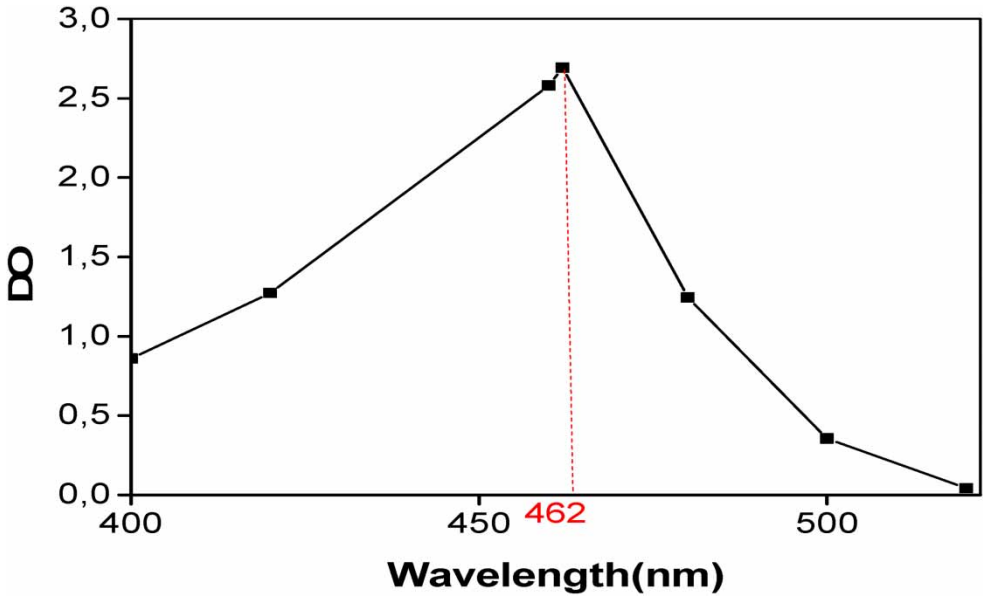

Figure 2 | Absorption spectrum of tartrazine.

A laser Raman microscope (LabRam HR, Horiba) with 600-nm wavelength was used to carry out Raman measurements. The spectra were recorded from 1,000 and 3,000 cm^{-1}. Powder X-ray diffraction (XRD) characterization has been used to determine the phase purity, grain size, and lattice space increment and decrease in the concentration of adsorbents. It is also often used to study the crystal defect of POAT, POAA, and POAS. The XRD patterns of all the samples were measured using a Bruker D8 Advance X-ray diffractometer with a rate of 5°/min at $\lambda = 1.55$ Å in the interval from 5° to 80°.

The role of the pH_{PZC} is to know the exact charge carried by the area of the adsorbent while adsorbing the dye. This corresponds to the pH value of the medium and the resultant charges (positive and negative) of the surface are zero. For this, 0.2 g of the adsorbent was added to 50 mL of 0.01 M NaCl for a pH range from 2 to 12 which will be adjusted by adding NaOH or HCl according to the Mahmood method (Mahmood *et al.* 2011). The bottle was closed and stirred at room temperature for 48 h in order to increase their final pH. The pattern of interception of the final pH (pH_f) according to the initial pH (pH_i) with bisector determines the pH_{PZC}.

For the equilibrium pH, 1 g of the adsorbent is dissolved in 100 mL of distilled water ($pH = 5.2 \pm 0.2$), stirred for 24 h and then allowed to stabilize and finally the measurements are taken after 25 min with a pH-meter (VOLTCRAFT).

2.5. Adsorption experiments

Various adsorption samples were prepared by batch systems by mixing 0.01 g of adsorbent with 50 mL of dye solutions at desired concentrations, and stirred at 300 rpm at given time intervals at ambient temperature (25 ± 2 °C), followed by filtration via Whatman filter paper to measure the residual tartrazine concentration by UV–Visible spectrophotometer (RAYLEIGH). The experiments were carried out at different times (5–40 min), masses (0.01–0.1 g), concentrations (10–40 mg/L), temperatures (298, 308, 318, and 328 K), and at different pH values (3–11).

The amount of dyes adsorbed per mg/g for POAT, POAA, and POAS at equilibrium, q_e (mg/g), is expressed by Equation (1) as follows (Dawood *et al.* 2017):

$$q_e(mg/g) = \frac{(C_i - C_e) \times V}{m} \quad (1)$$

where C_o is the initial concentration (mg/L), C_e is the concentration at equilibrium (mg/L), V is the volume used (L), and m is the mass used (g).

3. RESULTS AND DISCUSSION

3.1. Characterizations of adsorbent

3.1.1. Field emission scanning electron microscopy

FE-SEM micrographs of POAT, POAS, and POAA are shown in Figure 3. The external morphology of the POAT surface is different from that of orange peel chemically activated with acid (POAA) and soda (POAS). For POAT, we observed a smooth porous structure in the form of a less visible crane than for chemical activations, POAA has a very irregular rough structure in the form of a mound and is more porous than POAS and, therefore, a larger specific area justifies a better adsorption capacity (Sha *et al.* 2010). The determined specific areas of POAT, POAS, and POAA are 35.47, 49.70, and 65.74 $m^2.g^{-1}$ respectively.

3.1.2. Fourier transform infra-red spectroscopy

FTIR identifies the presence of any functional groups, and the results are shown in Figure 4. The IR spectra of our materials reveal five similar stretching vibration peaks and one deformation vibration as well as two peaks that make out POAT, POAS, and POAA. For similar peaks, we first have a sweeping tape in the part of 3,568–3,117 cm^{-1} assigned to the O–H (carboxyl, phenol, or alcohol) due to the acid characteristic of oranges. Secondly, the band observed at 2,915 cm^{-1} characterizes the aliphatic C–H vibration. Thirdly, the strip at 1,730 cm^{-1} suggests the existence of the C = O of carboxylic acids, esters, ketones, and aldehydes. Fourth, the strip in the 1,625–1,520 cm^{-1} region corresponds to the aromatic C = C group. Fifth, the strip at 1,033 cm^{-1} designed to the C–C bond and finally the strip 756 cm^{-1} corresponding to the deformation shudder of aromatic C–H bond in di- or tri-substituted. These results are in good agreement with the literature (Ma *et al.* 2014; Chukwuemeka *et al.* 2021; Abdelali 2022).

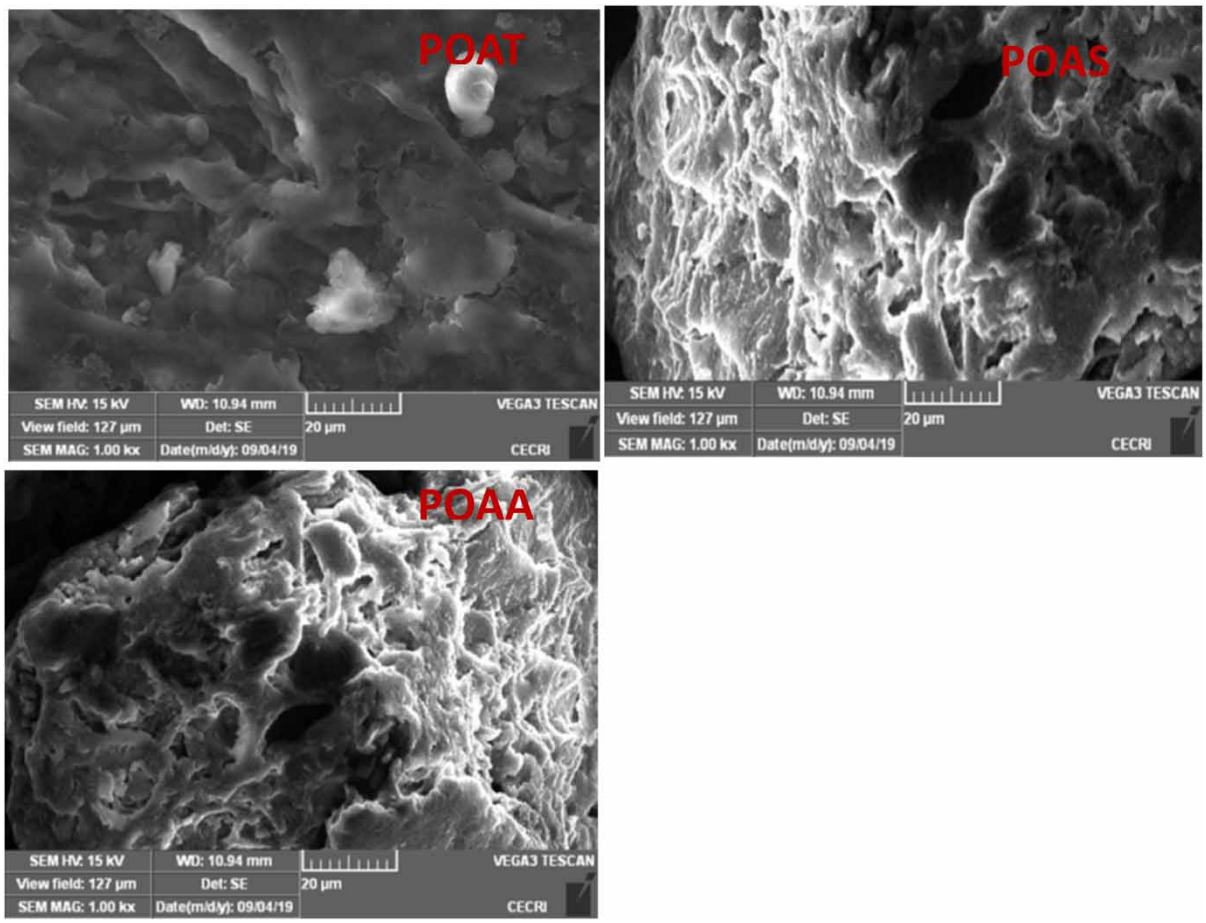

Figure 3 | FE-SEM micrographs of POAT, POAS, and POAA.

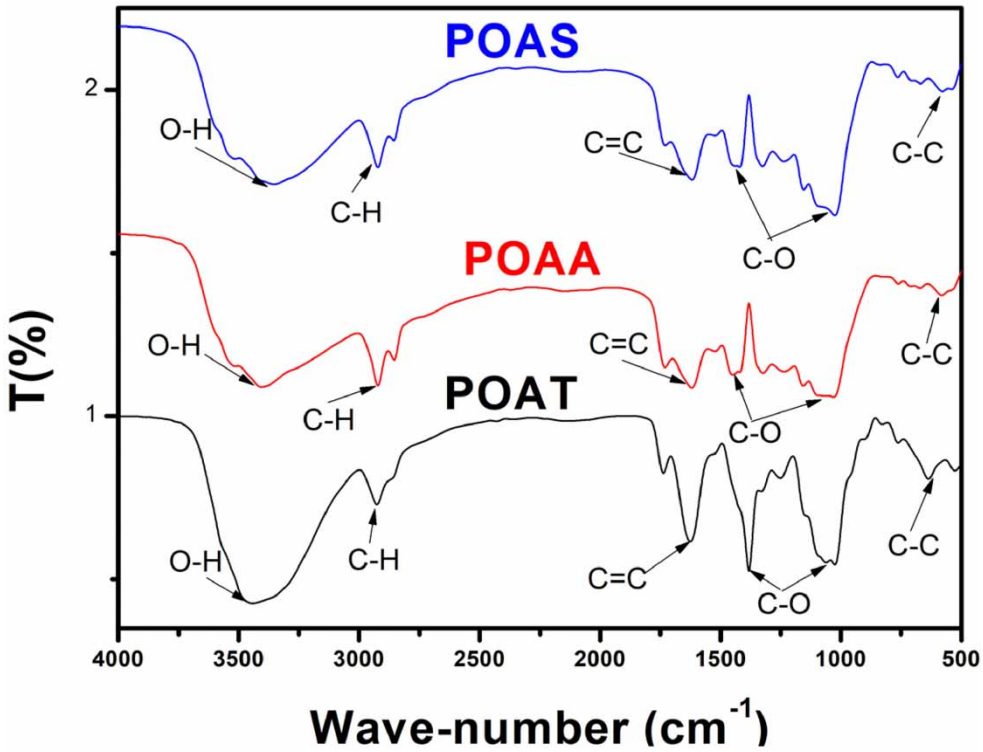

Figure 4 | FTIR spectrum of POAT, POAA, and POAS.

The peaks at 2,856 and 1,326 cm^{-1} correspond to the deformation of aliphatic C–H and C–O, respectively. The difference between the thermally treated adsorbent (POAT) and chemically treated adsorbents (POAS and POAA) is the reduction of the C–O bond of ester, ether, carboxylic acids, or alcohol in POAT while we have this bond in POAS and POAA. This is due to the activation temperature which has weakened the bonds present. Similar peaks are observed by Khormaei *et al.* (2007).

3.1.3. Raman spectroscopy and powder X-ray diffraction (XRD)

The vibrational characteristics were evaluated by Raman Spectroscopy and the results are presented in Figure 5. It can be found that the three materials exhibit three major peaks 1,347, 1,599, and 2,669 cm^{-1} which represent the band D, G, and 2D, respectively. The D-band denotes a defect/disorder in the carbon material, G-band is attributed to sp^2 carbon hybridization, and the 2D-band is the double Raman scattering by emission of two photons. The ratio of band intensities I_D/I_G is used to estimate the degrees of defect/disorder in our materials. The values of the intensity ratio of POAT (0.793) are smaller than POAA (0.913) and POAS (0.914), denoting that this sample contains less disorder in carbonaceous materials due to the deformation of the C–H groups. The XRD pattern showed the diffraction peaks 2θ at 24.20°, 25.51°, and 25.01° for POAT, POAS, and POAA, respectively, attributed to reflection in the plane of the graphitic structure (002). The peak around 42° is assigned to (100) which corresponds to a lower degree of graphitization and a higher degree of disorder which is a valuable property for very porous materials (Güzel 2017). The same remarks have been made previously by other researchers (Ma *et al.* 2014).

3.1.4. Dry matter, moisture, and ash tenor

It appears from the table that POAT has the highest dry matter content while its moisture and ash contents are low for the POAA and POAS. Our three adsorbents are well chosen because their ash content is low compared to those obtained by Torre Chauvin in 2015, and a low ash content indicates a good adsorbent and the high moisture content in POAA and POAS is due to the nature of activations (Table 1).

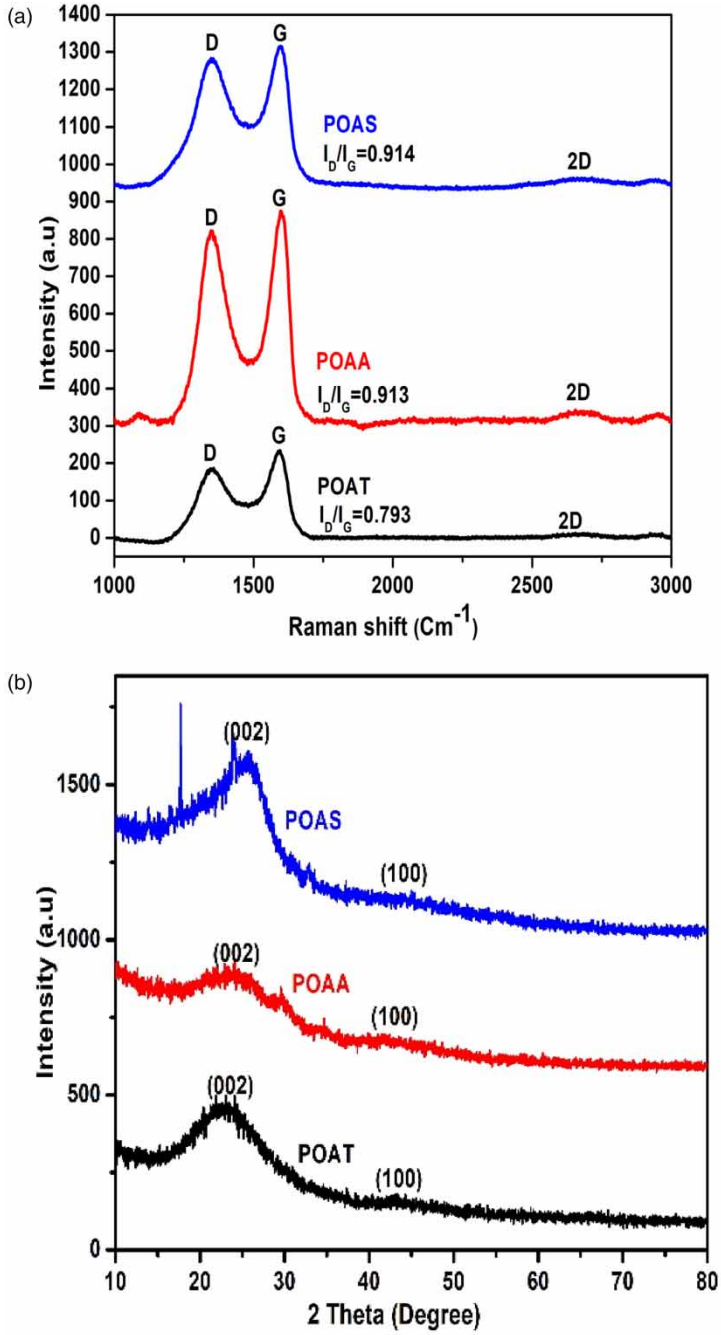

Figure 5 | Raman spectroscopy (a) and XRD (b) of POAT, POAA, and POAS.

3.1.5. Specific area, iodine index, equilibrium pH, and pH_{ZPC}

The specific surface of chemically activated adsorbents such as POAA (65.74 m^2/g) and POAS (49.70 m^2/g) is greater than that of thermally activated adsorbents, POAT (35.47 m^2/g). With regard to the values of a specific surface, we can say that chemical modification seems to improve the adsorption capacity of material more than thermal activation.

The values of the iodine number increase significantly as the activation temperature increases because the increase in temperature makes the micropores more available; hence, POAT contains more micropores than POAA and POAS. The value of the equilibrium pH of POAT is basic, whereas for POAA and POAS it is acidic; this is due to the way each support has been made (Table 2).

Table 1 | Values of dry matter, moisture, and ash tenor

Adsorbents	Dry matter (%)	Moisture content (%)	Ash content (%)
POAT	87.85 ± 11.58	12.15 ± 11.58	0.02 ± 0.01
POAA	73.21 ± 4.90	26.79 ± 4.90	0.13 ± 0.08
POAS	49.19 ± 0.81	50.81 ± 0.81	0.16 ± 0.12

Table 2 | Specific area, iodine indices, equilibrium pH, and pH_{zpc} of adsorbents

Adsorbents	Specific area (m^2/g)	Iodine index (mg/g)	pH	PH_{zpc}
POAT	35.47	753.82 ± 10.77	7.93 ± 0.03	9.15
POAA	65.74	468.28 ± 5.38	5.59 ± 0.03	6.88
POAS	49.70	441.63 ± 0.00	4.80 ± 0.02	4.50

3.2. Effect of contact time and initial concentration

To study the effect of contact time and initial concentration of dye on the removal capacity of dye solutions, the experiments have been carried out at a fixed mass (0.01 g), a pH of 6.60 for E102 at different concentrations (10–40 mg/L) and at different time intervals (5–40 min). It can be observed that the plateau formation time does not depend on the concentration and the quantity adsorbed increases with the concentration. As can be seen in Figure 6, the adsorption is rapid for the first 20 min for the support treated thermally and for the first 15 min for the support chemically treated with acid and soda before tending toward saturation by forming a plateau. This can be explained by the fact that, initially, the adsorption sites are vacant, hence there was a higher rate of adsorption, then the adsorption rate becomes slow due to the fact that the pores of our materials (Raphaël *et al.* 2020) are saturated by the dissolved species. The enhanced initial speed of adsorption with the initial concentration is higher (122.25 mg/g) for POAA than for POAT (121.74 mg/g) and POAS (116.35 mg/g) and is assigned to the elevation of the force of attraction between molecules and sites of adsorption. Moreover, the initial concentration provides strong forces for any resisting mass transfer between the species of aqueous solutions and the part of the adsorbent material (Haddad *et al.* 2014). These values are superior to those obtained by Domga *et al.* (2016) on Gudali Bones for a concentration of 60 mg/g (12.67 mg/g).

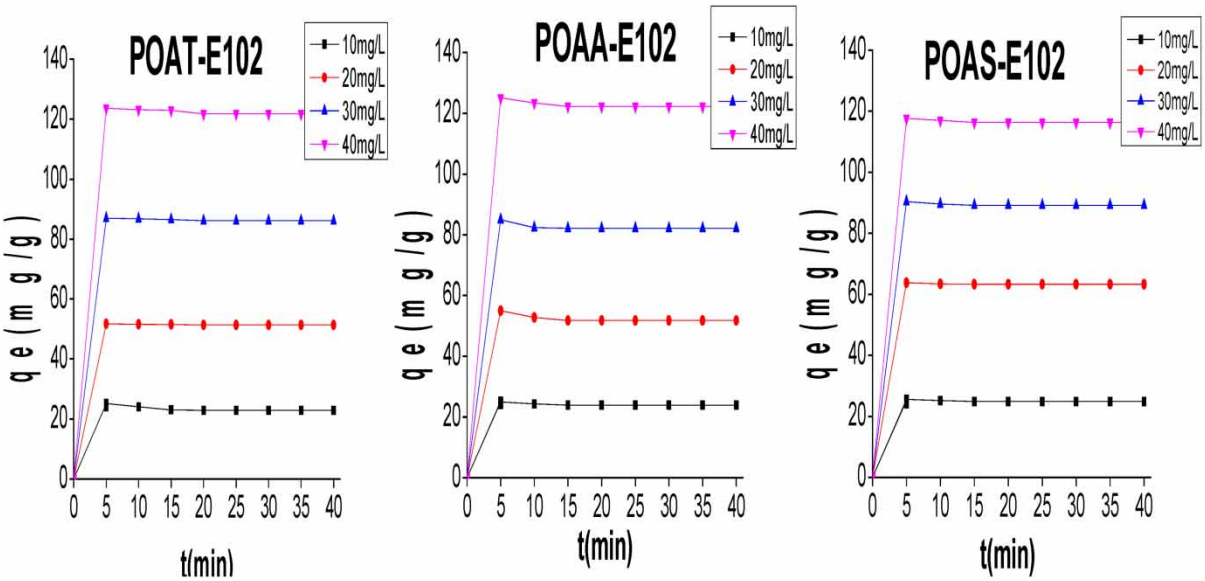

Figure 6 | Effect of contact time and concentration on the amount of tartrazine adsorbed onto POAT, POAA, and POAS.

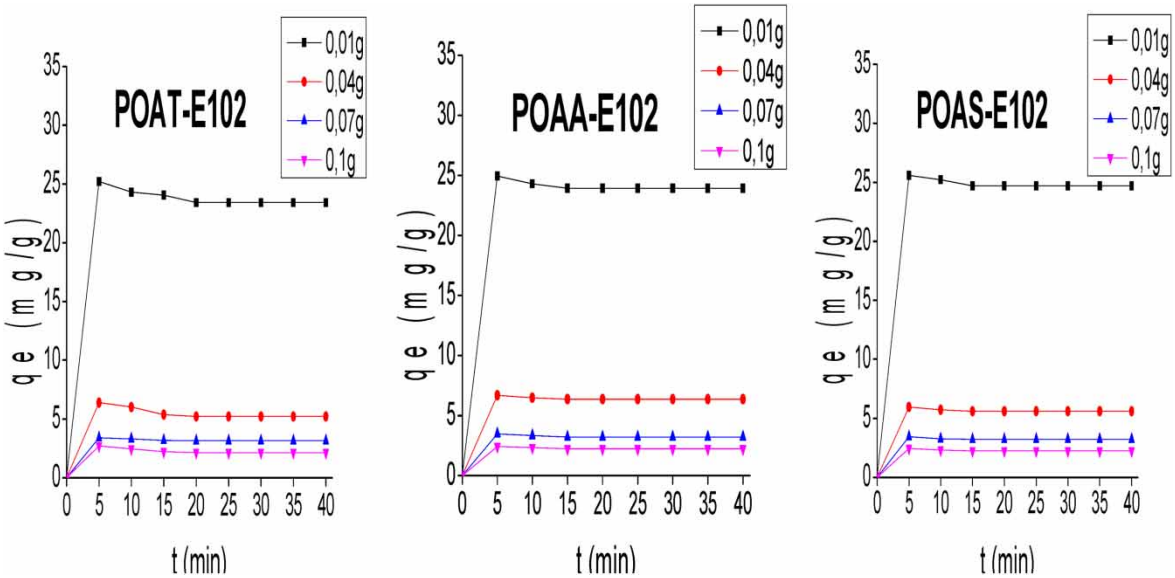

Figure 7 | Effect of adsorbent mass on to the amount of tartrazine adsorbed onto POAT, POAA, and POAS.

3.3. Effect of adsorbent mass

It is apparent from the figure that independent of the adsorbent used, the adsorbed amount of tartrazine decreases with increased mass (24.94–2.25 mg/g; 25.20–2.13 mg/g; and 25.58–2.23 mg/g, respectively), for POAA, POAT, and POAS due to the unsaturation of adsorption sites and the reciprocal influence between the molecules of the adsorbent which causes the desorption of the adsorbant from the small sites of the adsorbent (Wu *et al.* 2018). The same results are obtained by Harouna *et al.* (2020) and Abia *et al.* (2019). It can be concluded that POAS adsorbed more and the optimum mass of our three adsorbents is 0.01 g, and this mass was used for the rest of the study (Figure 7).

3.4. Effect of temperature

The effect of temperature has been studied in Figure 8. In view of these curves, the adsorption of E102 onto POAS, POAT, and POAA decreases with increasing temperature (25–55 °C), respectively, of 24.43–20.07 mg/g; 24.69–23.41 mg/g; and 27.64–25.33 mg/g, which suggests the adsorption is exothermic. This decrease in the quantity adsorbed is due to the action of the pore size since a significant part of the micropores at the same dimension as the molecule can only penetrate these pores under precise temperature conditions (Bembli *et al.* 2022). The same results were obtained by Abia *et al.* (2019) on the adsorption of Rhodamine B using orange peels.

3.5. Effect of pH

The pH is a key parameter to follow the adsorption process because it acts on the forms of the adsorbates in solution and on the possible charges of the surface of the adsorbents (Ma *et al.* 2014; Bembli *et al.* 2022) As shown in Figure 9, we observe that when the pH increases, the adsorbed amount of tartrazine decreases at optimal pH 3 and POAS (32.12 mg/g) adsorbed more than POAT (29.82 mg/g) and POAA (27.25 mg/g). The surface of POAT, POAA, and POAS is positively charged because the $pH < pH_{pzc}$ and E102 are negatively charged ($SOH_2^+ + Dye\text{-}SO_3^- \rightarrow Dye\text{-}SO_3^- SOH_2^+$). Beyond the optimum pH, the adsorption capacity decreases because the surface of our adsorbents becomes negatively charged and, therefore, the repulsion electrostatic between them can be favorable. The same results have been found by Raphaël *et al.* (2020) and Sousna *et al.* (2018).

3.6. Adsorption isotherm

In order to determine the adsorbate–adsorbent interaction, four suitable model isotherms were used, namely Langmuir, Freundlich, Temkin, and Dubinin-Redushkevic.

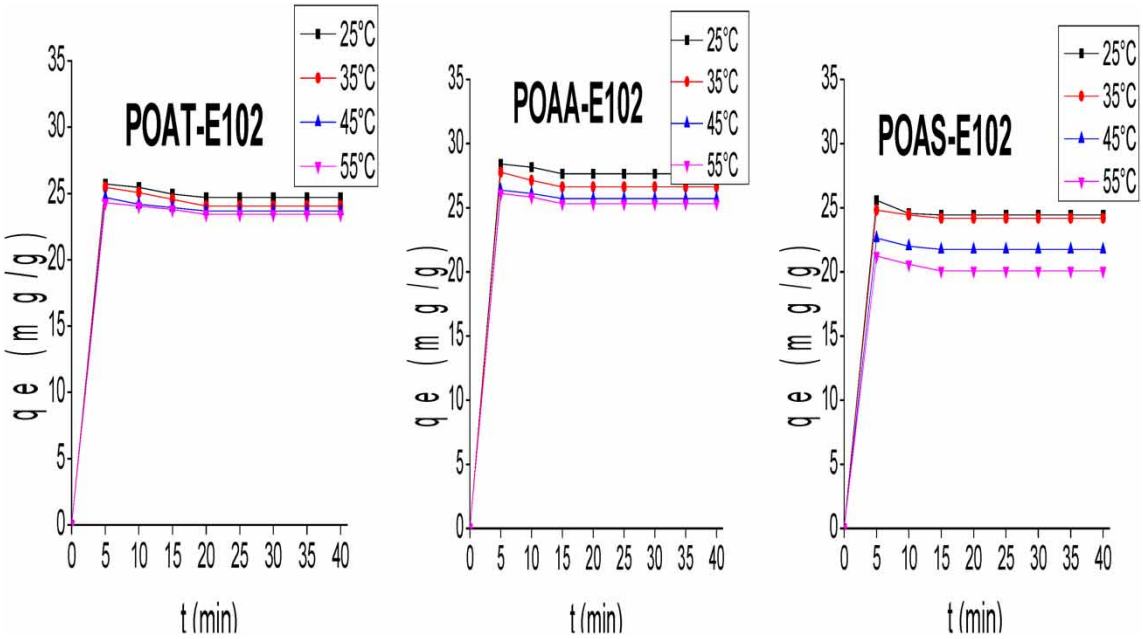

Figure 8 | Effect of temperature on the amount of tartrazine adsorbed onto POAT, POAA, and POAS.

3.6.1. Langmuir adsorption isotherm

The Langmuir model assumes that the surfaces of the adsorbent are homogeneous in terms of energy and does not take into account the interactions between the adsorbed molecules. Its equation is as follows:

$$\frac{C_e}{q_e} = \frac{C_e}{q_{\max}} + \frac{1}{KL.q_{\max}} \tag{2}$$

where C_e is the equilibrium concentration of the adsorbate (mg/L); q_e is the quantity of adsorbent at equilibrium (mg/g); $q_{\max}$ represents the maximum adsorption capacity (mg/g), and K_L is the Langmuir isotherm constant (L/mg).

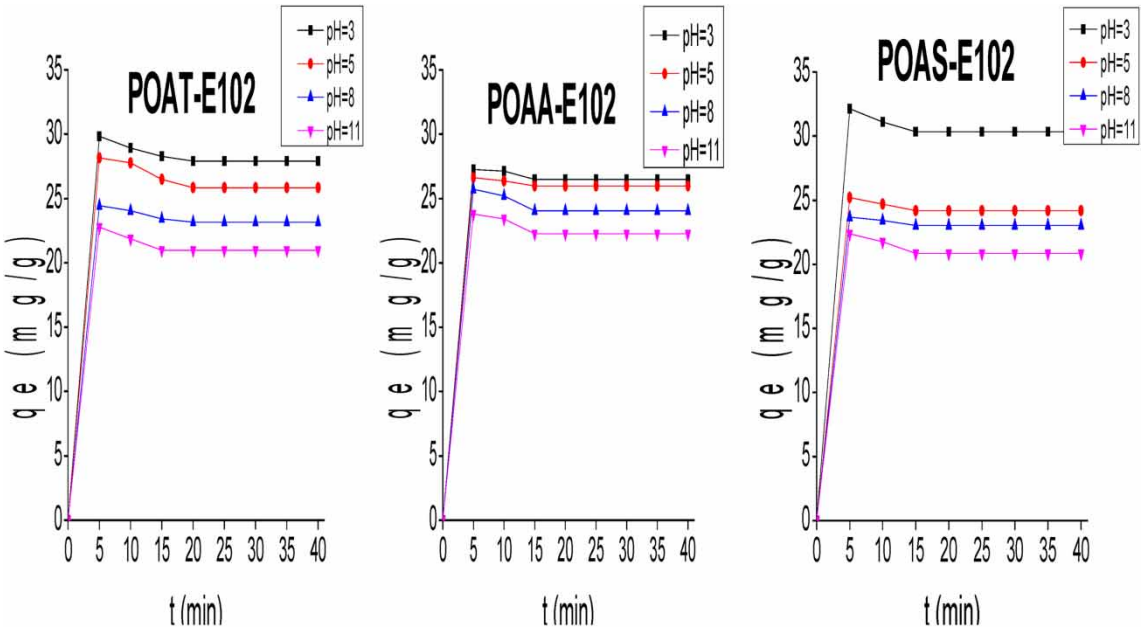

Figure 9 | Effect of pH on the amount of tartrazine adsorbed onto POAT, POAA, and POAS.

C_e/q_e in the function of C_e gives a straight line with $1/q_o$ as the slope and $1/q_{max}$. KL as the ordinate axis. To know if the adsorption is linear, irreversible, and favorable or not, the equilibrium parameter R_L was calculated by Equation (3) (Ho & Mckay 1998):

$$R_L = \frac{1}{1 + K_L.C_o} \tag{3}$$

where C_o is the greatest initial concentration of the dye (mg L^{-1}) $0 < R_L < 1$: favors adsorption; $R_L = 1$: linear; $R_L = 0$: irreversible and when RL > 1: unfavorable.

3.6.2. Freundlich adsorption isotherm

Freundlich presumes a heterogeneous surface of adsorbent with an exponential distribution of active sites as a function of adsorption energy. Its equation is represented by Rao *et al.* (2002):

$$\log q_e = \frac{1}{n} \log C_e + \log K_F \tag{4}$$

where q_e represents the quantity adsorbed at equilibrium (mg/g); C_e is the equilibrium concentration of the adsorbate (mg/L); K_F is the Freundlich constant; and n is the constant related to the intensity of adsorption associated with heterogeneity factor.

The plots of log q_e against log C_e should give a linear graph $n =$ slope; K_F is the intercept of the graph.

3.6.3. Temkin adsorption isotherm

This model considers a non-uniformity of surface and a preferential occupation of the most adsorbent sites.

The Temkin isothermal model is generally applied in the following:

$$q_e = \frac{R_T}{b} \ln\ (AC_e)\ or\ q_e = B \ln A + B \ln C \tag{5}$$

with $B = RT/b$, where q_e is the quantity adsorbed at equilibrium (mg/g), C_e is the equilibrium concentration of the adsorbate (mg/L); T is the temperature (K), R is the gas constant (8.314 J/mol/K), B and A are calculated from the slope (B) and intercept (B ln$A$) of the plot of q_e against lnC_e.

3.6.4. Dubinin-Radushkevic adsorption isotherm

It is based on the volume occupied using the application of Polanyi's potential theory, which assumes that the interactions between the adsorbate and the adsorbent are established by a potential field and the adsorbate volume is one of the function of the potential field ε.

The expression of the Dubinin-Redushkevich equation is as follows (Dubinin & Radushkevich 1947):

$$lnq_e = lnq_o - \beta\varepsilon^2 \tag{6}$$

where q_e (mg/g) is the quantity of E102 adsorbed; β is the relative constant of the adsorption energy, q_m is the theoretical capacity of the micropores, ε is the potential of Polanyi (ε: RTln $(1 + 1/C_e)$).

These results (Table 3) show that only Freudlich and Temkin isotherm models best explain the phenomenon of E102 adsorption on POAT, POAA, and POAS.

3.7. Adsorption kinetics

Pseudo-first- and second-order and intra-particle diffusion were employed to explain the kinetic adsorption process.

Lagergren has proposed this equation (Lagergren & Svenska 1898):

$$\log\ (q_e\ -\ q_t) = log\ q_e - \frac{t}{2.303} K_1 \tag{7}$$

Table 3 | Parameters for the Langmuir, Freundlich, Temkin, and Dubinin-Radushkevic

Isotherms	Parameters	POAT	POAA	POAS
Langmuir	q_{max} (mg/g)	−91.743	−125.000	−333.333
	K_L (L/mg)	−0.037	−0.030	−0.016
	R^2	0.989	0.949	0.174
Freundlich	N	0.635	0.705	0.829
	K_F (mg/g)	1.550	2.216	4.306
	R^2	0.994	0.983	0.904
Temkin	B	−60.116	−54.066	−63.544
	A	0.076	0.068	0.80
	R^2	0.999	0.999	0.999
Dubinin-Radushkevic	Q_o	$2.4\ 10^{32}$	$2.1\ 10^{34}$	$1.8\ 10^{-08}$
	B	0.0002	0.0002	−0.0008
	R^2	0.828	0.014	0.862

where K_1 is the rate constant (min^{-1}), q_e is the quantity adsorbed on the surface at equilibrium (mg/g), and q_t is the quantity adsorbed on the surface at the time (mg/g).

The values of K_1 and q_e are calculated and listed in Table 4.

Equation (8) is that of the second-order kinetic:

$$\frac{t}{q_t} = \frac{1}{K_2 q_e^2} + \frac{1}{q_e} t \tag{8}$$

K_2 (mg/g.min) is the second-order rate constant. The values of q_e and K_2 are listed in Table 4.

The Weber–Morris intra-particle diffusion model is determined using the following equation:

$$q_t = K_3 t^{1/2} + C' \tag{9}$$

where K_3 is the intra-particle diffusion rate constant ($mg/g.min^{-1/2}$) and C' is the intercept.

The parameters of the kinetic model of intraparticle scattering are shown in Table 4.

From the following results, we can conclude that only the pseudo-second model best describes the adsorption of tartrazine because the values of correlation coefficients R^2 are greater than 0.90 and its mechanism is two steps: the diffusion of E102 to the area and the interaction of the E102 molecules to the area of adsorbents.

Table 5 shows the comparison of the adsorption removal capacity of various orange peel powders treated differently for E102 with other reported materials. It is evident that POAT, POAA, and POAS displayed a better affinity for tartrazine than most of the materials utilized for tartrazine uptake such as bio-adsorbent, activated carbon, and ion-exchange resin.

Table 4 | Pseudo-first-order, pseudo-second, and intra-particle diffusion kinetic models

Models	Parameters	POAT	POAA	POAS
Pseudo-first-order	R^2	0.529	0.215	0.416
	K_1 (min^{-1})	−0.046	−0.043	−0.021
	$q_{e\ cal}$ (mg/g)	0.722	0.314	0.701
Pseudo-second-order	R^2	0.999	1	1
	K_2 (mg/g.min)	−0.155	−0.392	−0.374
	$q_{e\ cal}$ (mg/g)	22.675	23.809	24.630
Intra-particle diffusion	R^2	0.501	0.537	0.539
	K_3 ($mg/g.min^{-1/2}$)	$6.43\ 10^{02}$	$8.58\ 10^{02}$	$1.08\ 10^{03}$
	C'	$6.33\ 10^{09}$	$3.44\ 10^{09}$	$6.52\ 10^{09}$

Table 5 | Comparison of the adsorption removal capacity of POAT, POAA, and POAS for E102 elimination with other reported materials

Adsorbent	q_e (mg/g)	References
Hen feather	6.4×10^{-5}	Mittal *et al.* (2007)
Sawdust	4.71	Banerjee & Chattopadhyaya (2013)
Raw clay	2.43	Raphaël *et al.* (2020)
Bridged clay	2.64	Raphaël *et al.* (2020)
Bottom ash	1.01×10^{-5}	Kurup *et al.* (2006)
De-oiled soya	2.12×10^{-5}	Kurup *et al.* (2006)
Activated carbon from cassava sievate biomass	20.83	Chukwuemeka *et al.* (2021)
Activated carbon-based cola nut shells	21.59	Nguela *et al.* (2021)
Polystyrene anion exchange resins	9.94	Wawrzkiewicz & Hubicki (2009)
POAT	121.74	This work
POAA	122.25	This work
POAS	116.35	This work

This demonstrates the potential application of orange peel powder as a low-cost material for the efficient depollution of wastewater contaminated with tartrazine dye.

3.8. Thermodynamic parameters

Thermodynamic parameters such as free standard energy $\Delta G°$ (kJ/mol), standard enthalpy $\Delta H°$ (kJ/mol), and standard entropy ($\Delta S°$) (kJ/mol/K) were determined by carrying out adsorption at three different temperatures and using the following Van't Hoff equations:

$$\Delta rG^{\circ} = -R_T \ln K_c \tag{10}$$

$$K_c = \frac{q_e}{C_e} \tag{11}$$

$$\ln K_c = \frac{\Delta rS^{\circ}}{R} - \frac{\Delta rH^{\circ}}{R_T} \tag{12}$$

where K_c is the equilibrium constant; q_e (mg/g) is the quantity adsorbed; Ce (mg/L) represents the concentration of solution at equilibrium; R is the gas constant (8.314 J /mol/K); and T is the temperature (K). The results are shown in Table 6.

According to Table 6, the enthalpies $\Delta H°$ (kJ/K.mol) are shown as negative values, which implies that the elimination of E102 is exothermic and this reaction is spontaneous of physical type with all negative ΔrG° values. As for the values of $\Delta rS°$, we can say that there is a reduction at the interface of POAA and POAS which leads to a good organization of the E102 molecules at the level of the adsorption sites while this order increases in POAT.

4. CONCLUSION

This work investigated the utilization of low-cost adsorbents derived from POAT, POAA, and POAS for the elimination of tartrazine (E102) azo dyes from an aqueous solution. The surface characterization of adsorbents revealed the presence of

Table 6 | Thermodynamics parameters for the adsorption of E102

				$\Delta rG°$ (kJ/mol)			
Adsorbents	$\Delta rH°$ (kJ/mol)	$\Delta rS°$ (kJ/mol)	R^2	298	308	318	328
POAT	−1.087	0.002	0.999	−1.683	−1.705	−1.725	−1.743
POAA	−2.227	−0.0009	0.974	−1.959	−1.933	−1.913	−1.937
POAS	−4.410	−0.008	0.915	−2.278	−2.355	−2.431	−2.508

functional groups required for the removal of E102 by POAT, POAA, and POAS. The FE-SEM micrographs of adsorbents displayed porous structures which have specific chemical functions on their surface according to their nature of activation. During the study of different parameters like initial concentration, mass, temperature, and pH over time, the quantity adsorbed increases with concentration, whereas it decreases with mass, temperature, and pH. The optimal conditions for adsorption are as follows: concentration = 40 mg/L; mass = 0.01 g; temperature = 25 °C; pH = 3. The E102 adsorption process was better described by Freundlich and Temkin isotherm than Langmuir and Dubinin-Radushkevich, as well as the pseudo-second-order model. Furthermore, thermodynamic studies confirmed that the adsorption process was spontaneous, physical reaction, and exothermic. It can be concluded that the findings of this study show an efficient removal of E102 azo dyes using low-cost adsorbents (POAT, POAA, and POAS). This study can be extended for the removal of other dyes from various aqueous solutions. To complete this research, further work will be conducted to determine the mechanisms of tartrazine adsorption onto the adsorbents and investigate their adsorption/desorption isotherms.

DATA AVAILABILITY STATEMENT

All relevant data are available from an online repository or repositories.

CONFLICT OF INTEREST

The authors declare there is no conflict.

REFERENCES

Abdelali, O. 2022 *Removal Efficiency of Simple Organic Compounds by Physicochemical Surface Wastewater Treatment Processes. Thesis University of Ferhat Abbas-Setif 1*.

Abia, D., Amana, T. H., Noumi, G. B., Domga, R. & Domga 2019 Adsorption of Rhodamine B onto Orange Peel Powder. *American Journal of Chemistry* **9** (5), 142–149.

Arami, M., Yousefi, N., Mohammad, N. & Salman, N. 2006 Equilibrium and kinetics studies for the adsorption of direct and acid dyes from aqueous solution by soy meal hull. *Journal of Hazardous Materials* **135**, 171–179. https://doi.org/10.1016/j.jhazmat.2005.11.044.

Banerjee, S. & Chattopadhyaya, M. C. 2013 Adsorption characteristics for the removal of a toxic dye, tartrazine from aqueous solutions by a low cost agricultural by-product. *Arabian Journal of Chemistry*, 1–10. https://doi.org/10.1016/j.arabjc.2013.06.005.

Bembli, M., Zine, M., Bechrifa, A. & Boughzala, K. 2022 Study of the adsorption of Acid Red 52 by by-products of the phosphate industry. *RHAZES:Green and Applied Chemistry* **15**, 51–65.

Benaïssa, H. & Elouchdi, M. A. 2011 Biosorption of copper (II) ions from synthetic aqueous solutions by drying bed activated sludge. *Journal of Hazardous Materials Journal* **194**, 69–78. https://doi.org/10.1016/j.jhazmat.2011.07.063.

Benamraoui, F. 2014 *Elimination des colorants cationiques par des charbons actifs synthétisés à partir des résidus de l'agriculture*. Magister Faculté de Technologie Université Ferhat Abbas Setif.

Chukwuemeka, H. O., Francis, O., Kovo, K. E., Nnaji, J. C. & Okereafor, A. G. 2021 Adsorption of Tartrazine and sunset yellow anionic dyes onto activated carbon derived from Cassava Sievate biomass. *Applied Water Science* **11** (27), 1–8. https://doi.org/10.1007/s13201-021-01357-w.

Dawood, S., Sen, T. K. & Phan, C. 2017 Synthesis and characterisation of slow pyrolysis pine cone bio-char in the removal of organic and inorganic pollutants from aqueous solution by adsorption: kinetic, equilibrium, mechanism and thermodynamic. *Bioresource Technology* **246**, 76–81. https://doi.org/10.1016/j.biortech.2017.07.019.

Domga, R., Tcheka, C., Mouthe Anombogo, G. A., Kobbe-Dama, N., Domga, Tchatchueng, J. B., Tchigo, A. & Tsafam, A. 2016 Batch equilibrium adsorption of methyl orange from aqueous solution using animal activated carbon from Gudali Bones. *International Journal of Innovation Sciences and Research* **5** (7), 798–805.

Dubinin, M. M. & Radushkevich, L. V. 1947 Equation of the characteristic curve of activated charcoal. *Proceedings of the Academy of Sciences of the USSR, Physical Chemistry* **55**, 331–333.

Greluk, M. & Hubicki, Z. 2011 Efficient removal of acid orange 7 dye from water using the strongly basic anion exchange resin Amberlite IRA-958. *Desalination* **278** (1–3), 219–226. https://doi.org/10.1016/j.desal.2011.05.024.

Güzel, F. 2017 Novel and sustainable precursor for high-quality activated carbon preparation by conventional pyrolysis : optimization of produce conditions and feasibility in adsorption studies. *Advanced Powder Technology*, 1–11. https://doi.org/10.1016/j.apt.2017.12.014.

Haddad, K., Jellali, S., Jaouadi, S. & Benltifa, M. 2014 Raw and treated marble wastes reuse as Low cost materials for phosphorus removal from aqueous solutions : efficiencies and mechanisms. *Comptes Rendus Chimie*, 1–13. https://doi.org/10.1016/j.crci.2014.07.006.

Harouna, M., Djakba, R. & Mouhamadou, S. 2020 Adsorption of copper ions (Cu++) in aqueous solution using activated carbon and biosorbent from Indian Jujube (Ziziphus mauritiana) Seed Hulls. *Chem. Sci. Int. J.* **29**, 13–24.

Ho, Y. S. & Mckay, G. 1998 A comparison of chemisorption kinetic models applied to pollutant removal on various sorbents. *Process Safety and Environmental Protection* **76**, 332–340.

Khormaei, M., Nasernejad, B., Edrisi, M. & Eslamzadeh, T. 2007 Copper biosorption from aqueous solutions by sour orange residue. *Journal of Hazardous Materials* **149**, 269–274.

Kraemer, M. V., Fernandes, A. C., Chaddad, M. C., Uggioni, P. L., Rodrigues, V. M., Bernardo, G. L. & Proença, R. P. 2022 Food additives in childhood : a review on consumption and health consequences. *Revista de Saúde Pública* **56** (32), 1–22.

Kurup, L., Kurup, L., Ash, B. & Soya, D.-o. 2006 Adsorption isotherms, kinetics and column operations for the removal of hazardous Dye, tartrazine from aqueous S. *Journal of Hazardous Materials* **136**, 567–578. https://doi.org/10.1016/j.jhazmat.2005.12.037.

Lagergren, S. & Svenska, B. K. 1898 On the theory of so-called adsorption of materials. *Royal Swedish Academy of Sciences Doc., Band.* **24**, 1–13.

Ma, J., Shen, Y., Shen, C., Wen, Y. & Liu, W. 2014 Al-Doping chitosan – Fe (III) hydrogel for the removal of fluoride from aqueous solutions. *Chemical Engineering Journal* **248**, 98–106. https://doi.org/10.1016/j.cej.2014.02.098.

Mahmood, T., Saddique, M. T., Naeem, A., Westerho, P. & Mustafa, S. 2011 Comparison of different methods for the point of zero charge determination of NiO. *Industrial & Engineering Chemistry Research* **50**, 10017–10023.

Malik, R., Ramteke, D. S. & Wate, S. R. 2007 Adsorption of malachite green on groundnut shell waste based powdered activated carbon. *Waste Management* **27**, 1129–1138. https://doi.org/10.1016/j.wasman.2006.06.009.

Mittal, A., Kurup, L. & Mittal, J. 2007 Freundlich and Langmuir adsorption isotherms and kinetics for the removal of Tartrazine from aqueous solutions using Hen feathers. *Journal of Hazardous Materials* **146**, 243–248. https://doi.org/10.1016/j.jhazmat.2006.12.012.

Nguela, D., Brice, C., Manga, N. H., Arnold, B. S., Daouda, K., Victoire, A. A., Ndongo, N., Giresse, A., Nangah, C. R. & Nsami, N. J. 2021 Adsorption of tartrazine onto activated carbon based cola nuts shells : equilibrium, kinetics, and thermodynamics studies. *Open Journal of Inorganic Chemistry* **11**, 1–19. https://doi.org/10.4236/ojic.2021.111001.

Ollemberg, C. E. R. 2005 Simultaneous determination of food dyes by first derivative spectrophotometry with sorption onto polyurethane foam. *Analytical Sciences* **21**, 1–5.

Panel, E. & Chain, F. 2009 Scientific opinion on arsenic in food. *European Food Safety Authority* **7** (10), 1–199. https://doi.org/10.2903/j.efsa.2009.1351.

Pearce, C. I., Lloyd, J. R. & Guthrie, J. T. 2003 The removal of colour from textile wastewater using whole bacterial cells : a review. *Dyes and Pigments* **58**, 179–196. https://doi.org/10.1016/S0143-7208(03)00064-0.

Pereira, A., Balbani, S., Bardella, L. & Montovani, J. C. 2006 Excipientes de Medicamentos e as Informações Da Bula. *Revista Bras Otorrinolaringol* **72** (3), 400–406.

Ramuthai, S., Nandhakumars, V., Thiruchelvi, M., Arivoli, S. & Vijayakumaran, V. 2009 Rhodamine B adsorption- kinetic, mechanistic and thermodynamic studies. *E-Journal of Chemistry* **6**, 363–373.

Rao, M., Parwate, A. V. & Bhole, A. G. 2002 Removal of Cr (VI) and Ni (II) from aqueous solutions using bagasse and fly ash, waste management. *Waste Management* **22** (7), 821–830.

Raphaël, D., Massaï, H., Bagamla, W. & Talami, B. 2020 Study of the adsorption of methylene blue and tartrazine in aqueous solution by local materials of Cameroonian origin. *American Journal of Physical Chemistry* **9** (3), 45–51. https://doi.org/10.11648/j.ajpc.20200903.11.

Scotter, M. J. & Castle, L. 2004 Chemical interactions between additives in foodstuffs : a review. *Food Additives and Contaminants* **21** (2), 93–124. https://doi.org/10.1080/02652030310001636912.

Sha, L., Xue-yi, G. U. O., Ning-chuan, F. & Qing-hua, T. 2010 Effective removal of heavy metals from aqueous solutions by orange peel xanthate. *Transactions of Nonferrous Metals Society of China* **20**, s187–s191. https://doi.org/10.1016/S1003-6326(10)60037-4.

Sousna, S., Mokhtar, B., Chafia, T. & Abdelkrim, K. 2018 Adsorption of tartrazine from an aqueous solution by octadecyltrimethylammonium bromide-modified bentonite: Kinetics and isotherm modeling. *Comptes Rendus Chimie* **21** (3–4), 391–398. https://doi.org/10.1016/j.crci.2018.01.008.

Wawrzkiewicz, M. & Hubicki, Z. 2009 Removal of Tartrazine from aqueous solutions by strongly basic polystyrene anion exchange resins. *Journal of Hazardous Materials* **164**, 502–509. https://doi.org/10.1016/j.jhazmat.2008.08.021.

Wu, L., Wan, W., Shang, Z., Gao, X., Kobayashi, N., Luo, G. & Li, Z. 2018 Surface modification of phosphoric acid activated carbon by using non-thermal plasma for enhancement of Cu(II) adsorption from aqueous solutions. *Separation and Purification Technology*. https://doi.org/10.1016/j.seppur.2018.01.007.

First received 13 January 2023; accepted in revised form 29 June 2023. Available online 11 July 2023